Theoretical analysis of fluorescence signals in filamentation of femtosecond laser pulses in nitrogen molecular gas

E. Arévalo and A. Becker
Max-Planck-Institut für Physik Komplexer Systeme, Nöthnitzer Strasse 38, D-01187 Dresden, Germany
(Received 30 April 2005; revised manuscript received 1 August 2005; published 12 October 2005)

We study numerically and analytically the role of the combined effect of self-focusing, geometrical focusing, and the plasma defocusing in the formation of the fluorescence signal during the filamentation of a Ti:sapphire laser pulse in nitrogen molecular gas. Results of numerical simulations are used to estimate the number of excited ions in the focal volume, which is proportional to the fluorescence signal. We find good agreement between the theoretical results and the experimental data, showing that such data can be used to get further insight into the effective focal volume during filamentation of femtosecond laser pulses in transparent media.

DOI: 10.1103/PhysRevA.72.043807 PACS number(s): 42.65.Jx, 52.38.Hb, 32.80.Rm

I. INTRODUCTION

There has recently been considerable interest in the propagation of femtosecond (fs) laser pulses in gases undergoing multiphoton ionization. Experimental studies have shown that the defocusing effect of the resulting free-electron density combined with the Kerr self-focusing effect contribute to the formation of filaments when adequate high-power fs laser pulses propagate [1]. These filaments can range over large distances beyond the Rayleigh range of the laser pulse, from a few centimeter in solids or liquids up to a few kilometers in air [2]. This phenomenon is an active area of research not only in view of the possible applications such as the control of lightning discharge [3,4] and remote sensing [2,5,6], but also due to the complex dynamics during the propagation and filamentation process.

Due to the high intensities in the filament measurement systems cannot be incorporated into the beam and information has to be retrieved indirectly from observations of quantities from outside. There are a number possibilities in the experiments, among them are the detection of scattered light by a charge coupled device (CCD) camera or a photodiode [1,7,8], observations of beam patterns on linagraph print paper [9], fluorescence emission from excited molecules or ions [10,11], time-resolvent broadband absorption spectroscopy [6], measurement of the electric conduction of the plasma channel [12], observation of harmonic generation [13], or spectral interferometry [8].

Among these methods the observation of fluorescence from the nitrogen molecule or its ion has been shown to provide useful insights into the long distance propagation in air. Inside the filament nitrogen molecules are ionized, leaving the ion in its excited states with some probability. Fluorescence occurs either due to a radiative decay of the excited ions [14,15] or due to electron-ion recombination into an excited state of the neutral molecule and subsequent radiative decay [10]. Since the corresponding band systems (the first negative band in N_2^+ and the second positive band in N_2) are not masked by the rather low contribution from the supercontinuum spectrum the observation method is also called "clean fluorescence."

Up to now there is no attempt of a quantitative comparison between experimental observations of fluorescence spectra obtained from laser filaments in nitrogen molecular gas and analytical or numerical calculations. Such a study might be, however, helpful in understanding the potential of the clean fluorescence method beyond a qualitative visualization of the filamentation process. Below we investigate the combined effect of self- and geometrical focusing and plasma defocusing by analyzing fluorescence signals observed during the interaction of Ti:sapphire laser pulses with nitrogen molecular gas at different pressures [16]. To this end, we will compare predictions from numerical calculations, based on a propagation model, for the number of ions in the excited state, which is proportional to the fluorescence signal, with experimental data. We will show by results of a semianalytical theory how the signals can be used to get further insight into the size of the volume, in which the intensity is clamped down to a maximum value in the high-intensity core part of a laser filament.

II. NUMERICAL MODEL

The propagation of a linearly polarized laser beam in N_2 gas is described by the scalar wave equation

$$\partial_z^2 E + \Delta E - \frac{1}{c^2}\partial_t^2 D = \frac{4\pi}{c^2}\partial_t^2 P_{NL} + \frac{4\pi}{c^2}\partial_t J, \tag{1}$$

where electric field strength E and D are related by the usual dispersion relation as $D(\vec{r},\omega)=\epsilon(\omega)E(\vec{r},\omega)$, and $\epsilon(\omega)$ is the dielectric constant of N_2. $P_{NL}=\chi^{(3)}E^3$ is the nonlinear polarization, $\chi^{(3)}$ is the third order nonlinear susceptibility of the medium, and c is the speed of light. The strong interaction of the radiation field with the N_2 molecules generates an ion density through multiphoton ionization, that in the Drude model [17] is described as

$$J = e\sum_l N_l v_l. \tag{2}$$

where N_l is the number of N_2 ions in the electronic state l ($l=0$ stands for the ground state, $l=1$ for the first excited state, and so on). e is the electron charge and v_l is the ion drift velocity, which obeys the equation of motion for ions in the Drude model: $m_l\partial_t v_l = e\,E - m_l v_l/\tau$, where m_l is the mass

of the ion. By using the slowly varying envelope approximation Eq. (1) in the retarded coordinate frame ($t \rightarrow \tau = t - z/v_g$) reads

$$i\partial_\xi \mathcal{E} + \frac{1}{4}\Delta_\perp \mathcal{E} + \frac{L_D}{L_{NL}}|\mathcal{E}|^2\mathcal{E} - \frac{1}{4}\frac{L_D}{L_d}\left(\partial_\tau^2 \mathcal{E} + \frac{i}{3}\frac{L_d}{L_d'}\partial_\tau^3 \mathcal{E}\right) - \sum_l \frac{L_D}{L_{plas}^{(l)}}\rho_l \mathcal{E} + i\sum_l \frac{L_D}{L_{\mathrm{AP}}^{(l)}}\rho_l \mathcal{E} + i\sum_l \frac{L_D}{L_{\mathrm{MPA}}^{(l)}}|\mathcal{E}|^{2n_l-2}\mathcal{E} = 0, \tag{3}$$

where $\mathcal{E}$ is the electric field normalized to its initial maximum $\sqrt{I_0}$. n_l is the effective order of the ionization process and ρ_l is the number of N_2 ions in the electronic state l normalized to the initial number density of neutral atoms N_0, and obeys the relation

$$\rho_l = 1 - \exp\left(-T_0\sigma^{(n_l)}I_0^{n_l}\int_{-\infty}^{\tau}|\mathcal{E}|^{2n_l}d\tau\right). \tag{4}$$

Equation (3) has radial symmetry, in which the radius r and the time τ are given in units of length w_0 and duration T_0 of the laser pulse, respectively, the longitudinal coordinate ξ is given in units of the diffraction length scale $L_D = k_z w_0^2/2$. Other length scales are the dispersion length scales $L_d = T_0^2/2k_2$ and $L_{d'} = T_0^3/2k_3$, the nonlinear length scale $L_{NL} = 1/n_2 k_0 I_0$, the plasma length scale $L_{plas}^{(l)} = k_z m_l c^2/2\pi e^2 N_0$, the absorption-plasma length scale $L_{\mathrm{AP}}^{(l)} = m_l \omega_0 c^2 \tau_c k_z/2\pi e^2 N_0$, and the multiphoton-absorption length scale $L_{\mathrm{MPA}}^{(l)} = 2/n_l \hbar \omega_0 \sigma^{(n_l)} I_0^{n_l-1} N_0$. k_2 and k_3 are the second and third order group-velocity dispersion coefficients, respectively, and $\alpha_l = n_l \hbar \omega_0 N_0 \sigma^{(n_l)} I^{n_l-1}$ is the coefficient of multiphoton absorption by the molecules.

The model, described by Eq. (3), includes geometrical focusing, diffraction, group-velocity dispersion, self-focusing, and plasma generation via multiphoton ionization. For the numerical calculations we use parameters of the experiment [16] in order to make a comparison with the experimental data. We consider the propagation of a 800 nm laser pulse with pulse duration of 250 fs (FWHM) in nitrogen molecular gas. The critical power of N_2 is $P_{cr} = 3\ GW$ at atmospheric pressure. Note that P_{cr} varies with the inverse of the pressure. The density of neutral atoms is derived from the ideal gas law $N_0 = \Phi/k_B\Theta$, where Φ and Θ are pressure and temperature, respectively. We consider two values of pressure at room temperature ($\Theta = 300$ K), namely $\Phi = 400$ and 760 Torr. The multiphoton ionization transition rates were obtained by fitting the experimental data to the form $\sigma^{n_l}|\mathcal{E}|^2$, which is valid in the intensity range up to 2×10^{14} W/cm^2. It yields $\sigma^{(n_0)} = 4.45 \times 10^{-84}$ (cm^2/W)^{n_0} with $n_0 = 6.78$ [18], and $\sigma^{(n_2)} = 1.62 \times 10^{-108}$ (cm^2/W)^{n_2} with $n_2 = 8.32$ [15]. Note that ionization to the electronic ground state $l = 0$ is more dominant for the plasma generation than ionization to the excited states $l = 1$ and $l = 2$. But the fluorescence signal of the first negative band in N_2^+ is proportional to the total number of ions in the second excited state ($l = 2, B$ state). The contribution of the first excited state ($l = 1$) is hence negligible for the analysis. Finally, in the model we have used the second order and third dispersion group-velocity dispersion coefficient $k_2 = 0.2$ fs^2/cm and $k_3 = 0.1$ fs^3/cm, respectively, at $\lambda = 800$ nm.

III. COMPARISON OF NUMERICAL RESULTS WITH EXPERIMENTAL DATA

By observation of the fluorescence spectrum of nitrogen molecular gas, the phenomena of intensity clamping and refocusing were investigated [16]. To this end, pulses at 800 nm, 250 fs (FWHM) with energies of up to 100 mJ were focused by a 100 cm lens in an interaction chamber filled with N_2. Spectra were measured at different gas pressures and input laser energies. For the simulations, Eqs. (3) and (4) were solved using the Crank-Nicholson scheme [19] with the initial condition

$$\mathcal{E}(\xi = 0, r, \tau) = \mathcal{E}_0 \exp(-\tau^2)\exp[-(1 - ib_0)r^2]. \tag{5}$$

$b_0 = -1/\xi_F$ describes the initial wave front divergence of the laser pulse, where ξ_F is the focal length in units of L_D. The derivatives in time were solved exactly in frequency space by using a fast Fourier transform [19]. The temporal and radial form of $\mathcal{E}(r, \tau)$ was chosen to be a Gaussian with length $w_0 = 0.39$ cm and duration $T_0 = 212$ fs ($T_{\mathrm{FWHM}} = \sqrt{2 \ln 2} T_0 = 250$ fs). The complex pulse was represented on a regular grid with mesh size Δr and $\Delta\tau$. Typical grid sizes were $6w_0$ in the radial direction, $8T_0$ in the time domain and the $\Delta\xi$ step was chosen adaptive to ensure that the relative error of the on-axis intensity peak of the pulse did not exceed 10^{-6}. The beam convergence corresponds to the experimental situation, where a lens with focal length $f = 100$ cm was used.

As mentioned above, the fluorescence signal of the first negative band in nitrogen molecular ion is proportional to the total number of ions in the second excited state, namely:

$$S_{fluo} \approx N_{ion}^{(2)} = 2\pi \int_0^{\xi_F} d\xi \int_0^{\infty} r\, dr\, \rho_2(r, \tau = \infty). \tag{6}$$

In the present work we consider the plasma formation at the focal volume, i.e. up to the geometrical focusing point ξ_F.

In Fig. 1 we compare experimental data of the fluorescence signal of the first negative band in nitrogen molecular ion (open circles, [16]) with numerical results (solid squares) for the number of ions in the second excited state, $N_{ion}^{(2)}$, at two values of pressure, namely (a) 400 Torr and (b) 760 Torr. In both panels the experimental data (given in arbitrary units in [16]) are vertically scaled to match the numerical results at one point. The overall agreement between experimental data and numerical results below as well as above the critical power (near the change of slope in the data [16]) is good. We note, however, a deviation at 400 Torr (panel a) around the critical power.

This quantitative agreement puts us in the position to further analyze the experimental data in view of the size of the effective focal region in case of filamentation of the pulse, i.e., above the critical power for self-focusing. To this end, in the next section we use results from a variational approach to give an analytical estimation of the fluorescence signal.

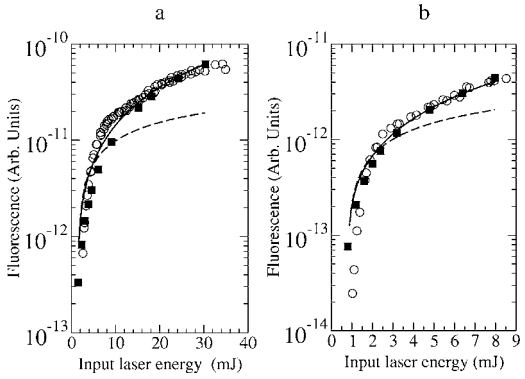

FIG. 1. Comparison of the experimental data of the fluorescence signal of the first negative band in nitrogen molecular ion (open circles, [16]) and the numerical predictions for the total number of ions in the second excited state (full squares) at (a) 400 Torr and (b) 760 Torr as a function the laser energy. The experimental data (given in arbitrary units) have been scaled vertically to match the numerical predictions; at one point, the x axis is unscaled. Also shown are the qualitative estimations from a variational approach (solid lines), Eq (6), and those assuming that the focal volume has cylindrical symmetry (dashed lines).

IV. ANALYTICAL ESTIMATION OF THE FLUORESCENCE SIGNAL

It has been shown [16] that the prominent change of slope in the fluorescence signal (c.f. Fig. 1) is due a clamping of the intensity inside the laser filaments. It has been further argued that the increase of the signal as a function of pulse energy after the change of slope is, therefore, an indication of the growth of the focal volume, in which the intensity is clamped down. Thus, above the critical power for self-focusing the fluorescence signal should be proportional to this effective focal volume V_{foc}:

$$S_{fluo} \approx V_{foc} = 2\pi \int_{\xi_{start}}^{\xi_{end}} d\xi \int_0^{r_{foc}(\xi)} r\, dr, \tag{7}$$

where ξ_{start} and ξ_{end} are the limits of the effective focal volume in propagation direction and $r_{foc}(\xi)$ is its radius at a given ξ.

The focal volume can be estimated as follows: First, we observe from the numerical simulations (c.f. Fig. 2) that above the critical power for self-focusing the on-axis intensity is clamped down to a maximum value between the self-focusing point $\xi_{start}=\xi_{SF}$, and the geometrical focus $\xi_{end}=\xi_F$, which determines the limits along the propagation direction. What is left is an estimation of $r_{foc}(\xi)$. One may assume that the width of the volume is approximately constant between self-focusing and geometrical focusing points. An estimation based on this assumption together with Marburger's formula for the self-focusing [20], however, does not give the trend of the numerical and exerimental results, as it can be seen in Fig. 1 (dashed line). Therefore, an alternative formalism is needed.

Instead we make use of the moving focusing model [21] combined with results of a variational approach to estimate $r_{foc}(\xi)$. According to the moving focusing model a laser pulse in the retarded frame can be viewed as a stack of transverse slices, each of which has an infinitesimal pulse duration and a power determined by the specific retarded time τ. Each pulse slice self-focuses to a singular focus depending on the value of its own power. The succession of foci can be thought of as a moving focus and generate the filament up to the geometrical focus. Based on this model we use a variational approach [22] to estimate the self-focusing distance and the width. In this approach the low-intensity outer part of the pulse [23], also called energy reservoir [24,25], is taken into account via a phase correction. It has been shown to provide an improved agreement with results from numerical simulations for the self-focusing distance and the width of the pulse during self-focusing process than earlier theories (e.g. [18,20,26,27]), in which the effect of the outer component of the pulse has been not considered. As an example we present in Fig. 3 a comparison between the semi-analytical estimates (line) and the results of numerical simulations (circles) for the self-focusing distance as a function of the laser power (scaled in units of the critical power) using the parameters of the experiment. In order to enhance the readability of the paper we outline the derivation of the variational approach in the Appendix and use here the results for

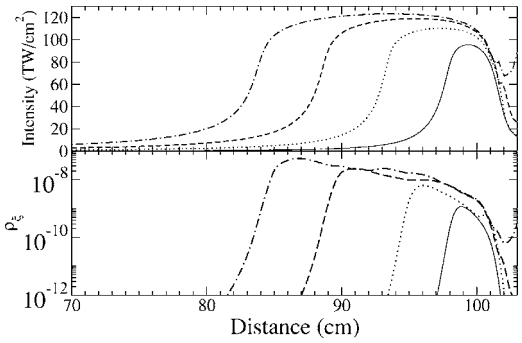

FIG. 2. Upper panel: On-axis intensity distribution, lower panel: $\rho_\xi = 2\pi \int_0^\infty dr\, r\rho_2(r,\xi,\tau=\infty)$ along the propagation axis for $\mathcal{P}=1$ (solid lines), $\mathcal{P}=4$ (dotted lines), $\mathcal{P}=5$ (dashed lines), and $\mathcal{P}=20$ (dot-dashed lines) at a pressure of 400 Torr.

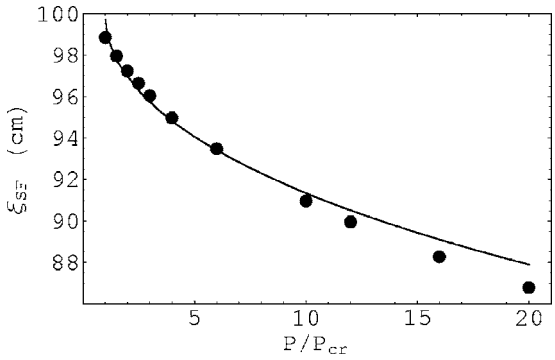

FIG. 3. Self-focusing distance ξ_{SF} as a function of the laser power $\mathcal{P}=P/P_{cr}$: Estimates of a variational approach [Eq. (A7), solid line] are compared with results of numerical simulations (circles). The self-focusing distance in the simulations is defined as the location of the first maximum of the plasma density. Parameters: Pressure of 400 Torr and geometrical focus at 100 cm.

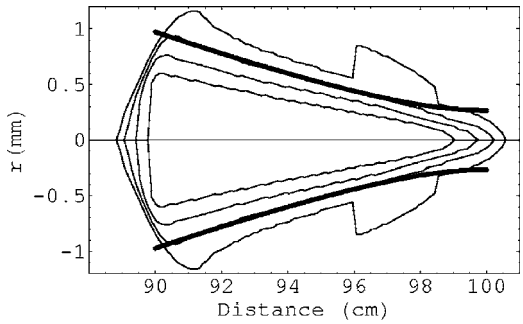

FIG. 4. Contour plot of the distribution of the number of N_2 ions in the B state ($l=2$), ρ_2, between the self-focusing and the geometrical focusing points. The four contours (thin lines) from outside to inside correspond to 19%, 37%, 56%, and 74% of the maximum of ρ_2. The theoretical prediction r_{foc} [thick lines, Eq. (8)] is multiplied by a factor 1.9 to fit the width at $1/e$ of the maximum (37% contour). Pressure of 400 Torr, geometrical focus at 100 cm and $\mathcal{P}=20$.

the self-focusing distance and the width $r_{foc}(\xi)$ of the focal volume beyond the self-focus.

Taking into account that $r_{foc}(\xi)=a(\xi)/\sqrt{2n_2}$, where n_2 is the effective order of the ionization process to the B state ($l=2$), together with the variational estimation of the width of the laser pulse at the self-focus, Eq. (A6), and the self-focusing distance Eq. (A7), we get

$$r_{foc}(\xi)=\left(\frac{1}{8\sqrt{n_2}}\right)\left(\frac{2^{-1-n_0}(L_D/L_{NL})^{n_0}(1+n_0)^2}{(L_D/L_{plas}^{(0)})g_0}\right)^{1/(2-2n_0)} \times\sqrt{32+9\left(\frac{1}{\xi}-\frac{1}{\xi_F}\right)^2}, \tag{8}$$

where g_0 is given by Eq. (A4).

The comparison of $r_{foc}(\xi)$ with contour plots of ρ_2 from numerical simulations is presented in Fig. 4, it shows a cone-like shape of the focal volume along the propagation axis (and not a constant radius as assumed above). We note that similar contour plots have been observed in numerical simulations for the case of twin laser pulses propagating in air [28]. Note also that there is no sign of rapid oscillatory pulse widths as predicted by other analytical methods [21,22].

Using Eq. (8) in Eq. (7) we get as a semianalytical expression for the focal volume:

$$V_{foc}=\frac{\pi}{64n_2}\left(\frac{2^{-1-n_0}(L_D/L_{NL})^{n_0}(1+n_0)^2}{(L_D/L_{plas}^{(0)})g_0}\right)^{1/(1-n_0)} \times\left[9\left(\frac{1}{\xi_{SF}}-\frac{1}{\xi_F}\right)+\left(32+\frac{9}{\xi_F^2}\right)(\xi_F-\xi_{SF}) -\frac{18}{\xi_F}\ln\left(\frac{\xi_F}{\xi_{SF}}\right)\right]. \tag{9}$$

In Fig. 1 the results of Eq. (9) are plotted as lines, showing a good relative agreement with the numerical results and the experimental data.

V. CONCLUSIONS

We have studied numerically and analytically experimental data of fluorescence spectra generated due to the interaction of nitrogen molecular gas with a short focused Ti:sapphire laser pulse at different gas pressures and pulse energies. To this end we have used a model for nonlinear pulse propagation in gaseous media to perform numerical simulations in a focusing geometry. We have calculated the total number of ions generated in an excited state, which is proportional to the observed fluorescence signal. We have also used an analytical method to estimate the focal volume during filamentation, in which the intensity is clamped down to a maximum value. Results of both, numerical simulations and semianalytical approach, are in good agreement with the experimental data, showing that an analysis of the fluorescence signal provides useful insight into the size of the effective focal volume during filamentation of the pulse.

APPENDIX: VARIATIONAL APPROACH

We use the ansatz

$$\mathcal{E}(\xi,r,\tau)=\frac{\mathcal{A}(\xi,\tau)}{a(\xi,\tau)}\exp\left(-\frac{r^2}{a^2(\xi,\tau)}\right) \times\exp\left(i\frac{b_0}{a(\xi,\tau)}r^2\right)\exp[i\phi(\xi,\tau)] \times\exp\{-ia(\xi,\tau)b(\xi,\tau)[\exp(-2r^2) -2r^2\exp(-2r^2)]\} \tag{A1}$$

for the electric field envelope, where $\mathcal{A}$ is the amplitude of the laser pulse, a is the pulse width, b_0 describes the initial wave front divergence (i.e. for collimated pulse $b_0=0$ or $b_0=-1/\xi_F$ for the case of a lens with focal length ξ_F), ϕ is a phase, and b is a coefficient multiplying a phase correction. The ansatz (A1) has been used before [22], but without taking into account multiphoton ionization. Here we extend the theory and derive a semianalytical expression for the width of the laser pulse at the self-focus in the presence of multiphoton ionization.

First we approximate Eq. (4) in the case of high pressures (>1 Torr) by

$$\rho_l=T_0\sigma^{(n_l)}I_0^{n_l}\int_{-\infty}^{\tau}|\mathcal{E}|^{2n_l}d\tau\ll 1, \tag{A2}$$

which can be integrated by using a simple integration rule up to the peak of the pulse [18], as

$$\rho_l=g_l(\tau)|\mathcal{E}|^{2n_l}, \tag{A3}$$

where

$$g_l(\tau)=\frac{\tau_{min}+\tau}{2}T_0\sigma^{(n_l)}I_0^{n_l}. \tag{A4}$$

Here τ_{min} is a cutoff determined by the initial pulse. Since the group-velocity dispersion is negligible for propagation of the pulse up to the self-focusing distance and, furthermore, one can show that for laser powers above the critical power $L_{NL}\ll L_d<L_{d'}$, one gets for Eq. (3)

$$i\partial_\xi \mathcal{E} + \frac{1}{4}\Delta_\perp \mathcal{E} + \frac{L_D}{L_{NL}}|\mathcal{E}|^2\mathcal{E} - \sum_l \frac{L_D}{L_{plas}^{(l)}} g_l(\tau)|\mathcal{E}|^{2n_l}\mathcal{E} + i\sum_l \left(\frac{L_D}{L_{\mathrm{AP}}^{(l)}} g_l(\tau)|\mathcal{E}|^{2n_l} + \frac{L_D}{L_{\mathrm{MPA}}^{(l)}}|\mathcal{E}|^{2n_l-2}\right)\mathcal{E} = 0. \quad \text{(A5)}$$

Equation (A5) can be derived from the Lagrange equation in the presence of losses. By following similar procedure as done in Refs. [29,18], we get a set of ordinary differential equations in ξ for the variables $\mathcal{A}$, a, b, ϕ. Using the initial conditions, $b(\xi=0)=0$, $a(\xi=0)=1$, and $\partial_\xi a(\xi=0)=b_0$ one gets the width of the pulse at the self-focus as

$$a_{min} = a(\xi = \xi_{SF}) = \frac{2^{(1+n_0)/[2(n_0-1)]}(L_D/L_{NL})^{n_0/[2(1-n_0)]}(n_0+1)^{1/(1-n_0)}}{(L_D/L_{plas}^{(0)})^{1/[2(1-n_0)]} g_l^{1/[2(1-n_0)]}}\sqrt{\mathcal{P}}. \quad \text{(A6)}$$

For the calculation of Eq. (A6) we have considered the contribution of the ground state ($l=0$) only, since the contributions of the excited states ($l>0$) are negligible.

In the case of no losses ($L_{\mathrm{AP}}^{(l)}\to\infty$ and $L_{\mathrm{MPA}}^{(l)}\to\infty$), and neglecting the ionization ($L_{plas}^{(l)}\to\infty$), one can derive an expression for the self-focusing distance [22], namely

$$\xi_{SF} = \frac{1}{\sqrt{\frac{32(\mathcal{P}-1)}{9}} - b_0}, \quad \text{(A7)}$$

where

$$\mathcal{P}(\xi,\tau) = \frac{2\pi}{P_{cr}}\int_0^\infty |\mathcal{E}|^2 r\, dr = \frac{\pi}{2P_{cr}}\mathcal{A}^2(\xi,\tau). \quad \text{(A8)}$$

In Eq. (A8) the critical power $P_{cr}=\pi L_{NL}L_D$.

[1] A. Braun, G. Korn, X. Liu, D. Du, J. Squier, and G. Mourou, Opt. Lett. **20**, 73 (1995).

[2] J. Kasparian, M. Rodriguez, G. Méjean, J. Yu, E. Salmon, H. Wille, R. Bourayou, S. Frey, Y.-B. André, A. Mysyrowicz, R. Sauerbrey, J. P. Wolf, and L. Wöste, Science **301**, 61 (2003).

[3] X. M. Zhao, J.-C. Diels, C. V. Wang, and J. M. Elizondo, IEEE J. Quantum Electron. **QE31**, 599 (1995).

[4] X. M. Zhao, S. Diddams, and J.-C. Diels, in *Tunable Laser Applications*, edited by F. J. Duarte (Marcel Dekker, New York, 1995), p. 113.

[5] L. Wöste, C. Wedekind, H. Wille, P. Rairoux, B. Stein, S. Nikolov, C. Werner, S. Niedermeier, F. Ronneberger, H. Schillinger, and R. Sauerbrey, Laser Optoelektron. **29**, 51 (1997).

[6] R. Rairoux, H. Schillinger, S. Niedermeier, M. Rodriguez, F. Ronneberger, R. Sauerbrey, B. Stein, D. Weite, C. Wedekind, H. Wille, L. Wöste, and C. Ziener, Appl. Phys. B: Lasers Opt. **71**, 573 (2000).

[7] E. T. J. Nibbering, P. F. Curley, G. Grillon, B. S. Prade, M. A. Franco, F. Salin, and A. Mysyrowicz, Opt. Lett. **21**, 62 (1996).

[8] B. La Fontaine, F. Vidal, Z. Jiang, C. Y. Chien, D. Comtois, A. Desparois, T. W. Johnston, J.-C. Kieffer, H. Pépin, and H. P. Mercure, Phys. Plasmas **6**, 1615 (1999).

[9] A. Brodeur, C. Y. Chien, F. A. Ilkov, S. L. Chin, O. G. Kosareva, and V. P. Kandilov, Opt. Lett. **22**, 304 (1997).

[10] A. Talebpour, M. Abdel-Faiteh, and S. L. Chin, Opt. Commun. **183**, 479 (2000).

[11] N. Kortsalioudakis, M. Tatarakis, N. Vakakis, S. D. Moustaizis, M. Franco, B. Prade, A. Mysyrowicz, N. A. Papadogiannis, A. Couairon, and S. Tzortzakis, Appl. Phys. B: Lasers Opt. **80**, 211 (2005).

[12] S. Tzortzakis, M. A. Franco, Y.-B. André, A. Chiron, B. Lamouroux, B. S. Prade, and A. Mysyrowicz, Phys. Rev. E **60**, R3505 (1999).

[13] H. R. Lange, A. Chiron, J.-F. Ripoche, A. Mysyrowicz, P. Breger, and P. Agostini, Phys. Rev. Lett. **81**, 1611 (1998).

[14] A. Talebpour, A. D. Bandrauk, J. Yang, and S. L. Chin, Chem. Phys. Lett. **313**, 789 (1999).

[15] A. Becker, A. D. Bandrauk, and S. L. Chin, Chem. Phys. Lett. **343**, 345 (2001).

[16] A. Becker, N. Aközbek, K. Vijayalakshmi, E. Oral, C. M. Bowden, and S. L. Chin, Appl. Phys. B: Lasers Opt. **73**, 287 (2001).

[17] R. W. Boyd, *Nonlinear Optics*, 2nd ed. (Academic Press, Boston, 2003).

[18] N. Aközbek, C. M. Bowden, A. Talebpour, and S. L. Chin, Phys. Rev. E **61**, 4540 (2000).

[19] W. H. Press, S. A. Teukolsky, W. T. Vetterling, and B. P. Flannery, *Numerical Recipes in Fortran*, 2nd ed. (Cambridge University Press, New York, 1994).

[20] J. H. Marburger, Prog. Quantum Electron. **4**, 35 (1975).

[21] A. Brodeur, C. Y. Chien, F. A. Ilkov, S. L. Chin, O. G. Kosareva, and V. P. Kandidov, Opt. Lett. **22**, 304 (1997).

[22] E. Arévalo and A. Becker, Phys. Rev. E **72**, 026605 (2005).

[23] G. Fibich and G. Papanicolaou, SIAM J. Appl. Math. **60**, 183 (1999).

[24] M. Mlejnek, E. M. Wright, and J. V. Moloney, Opt. Lett. **23**, 382 (1998).

[25] M. Mlejnek, M. Kolesik, J. V. Moloney, and E. M. Wright, Phys. Rev. Lett. **83**, 2938 (1999).

[26] J. Schwarz and J. C. Diels, Phys. Rev. A **65**, 013806 (2001).

[27] P. Sprangle, J. R. Peñano, and B. Hafizi, Phys. Rev. E **66**, 046418 (2002).

[28] A. Couairon, G. Méchain, S. Tzortzakis, M. Franco, B. Lamouroux, B. Prade, and A. Mysyrowicz, Opt. Commun. **225**, 177 (2003).

[29] S. C. Cerda, S. B. Cavalcanti, and J. M. Hickmann, Eur. Phys. J. D **1**, 313 (1998).